

各向异性表面张力对定向凝固中共晶生长形态稳定性的影响

徐小花 陈明文 王自东

Effect of anisotropic surface tension on morphological stability of lamellar eutectic growth in directional solidification

Xu Xiao-Hua Chen Ming-Wen Wang Zi-Dong

引用信息 Citation: [Acta Physica Sinica](#), 67, 118103 (2018) DOI: 10.7498/aps.67.20180186

在线阅读 View online: <http://dx.doi.org/10.7498/aps.67.20180186>

当期内容 View table of contents: <http://wulixb.iphy.ac.cn/CN/Y2018/V67/I11>

您可能感兴趣的其他文章

Articles you may be interested in

[BCC 枝晶生长原子堆垛过程的晶体相场研究](#)

Investigation of atom-attaching process of three-dimensional body-center-cubic dendritic growth by phase-field crystal model

物理学报.2015, 64(2): 028102 <http://dx.doi.org/10.7498/aps.64.028102>

[晶体相场法研究晶粒缩小过程中的位错湮灭与晶界迁移](#)

Phase-field crystal method investigated the dislocation annihilation and grain boundary migration in grain shrink process

物理学报.2014, 63(12): 128101 <http://dx.doi.org/10.7498/aps.63.128101>

[各向异性表面张力对定向凝固中深胞晶生长的影响](#)

Effect of anisotropic surface tension on deep cellular crystal growth in directional solidification

物理学报.2014, 63(3): 038101 <http://dx.doi.org/10.7498/aps.63.038101>

[基于改进元胞自动机模型的三元合金枝晶生长的数值模拟](#)

Simulation of dendritic growth for ternary alloys based on modified cellular automaton model

物理学报.2012, 61(10): 108101 <http://dx.doi.org/10.7498/aps.61.108101>

[茈四甲酸二酐有机单晶纳米结构的制备及形成机理的研究](#)

Preparation and investigation of the formation mechanism of organic single crystal nanostructures of PTCDA

物理学报.2012, 61(7): 078103 <http://dx.doi.org/10.7498/aps.61.078103>

各向异性表面张力对定向凝固中共晶生长形态稳定性的影响*

徐小花¹⁾ 陈明文^{1)†} 王自东^{2)‡}

1)(北京科技大学数理学院, 北京 100083)

2)(北京科技大学材料科学与工程学院, 北京 100083)

(2018年1月25日收到; 2018年3月15日收到修改稿)

研究各向异性表面张力对定向凝固中共晶生长形态稳定性的影响. 应用多重变量展开法导出了共晶界面表达式和扰动振幅的变化率满足的色散关系. 结果表明, 共晶生长系统有两种整体不稳定性机理: 由非震荡导致的“交换稳定性”机理和由震荡导致的“整体波动不稳定性”机理. 震荡有四种典型模式, 即: 反对称-反对称(AA-), 对称-反对称(SA-), 反对称-对称(AS-)和对称-对称(SS-)模式. 稳定性分析表明: 共晶界面形态稳定性取决于Peclet数 ε 的某一个临界值 ε_* , 当 ε 大于临界值 ε_* 时, 共晶界面形态不稳定; 当 ε 小于临界值 ε_* 时, 共晶界面形态稳定. 随着各向异性表面张力增大, 对应于AA-, SA-和SS-模式的临界值 ε_{aa*} , ε_{sa*} 和 ε_{ss*} 随之减小, 表明各向异性表面张力减小这三种模式的稳定性区域; 然而, 随着各向异性表面张力增大, 对应于AS-模式的临界值 ε_{as*} 随之增大, 表明各向异性表面张力增大AS-模式的稳定性区域.

关键词: 定向凝固, 共晶生长, 各向异性表面张力, 形态稳定性

PACS: 81.10.Aj, 68.03.Cd, 68.08.-p, 81.30.Fb

DOI: 10.7498/aps.67.20180186

1 引言

共晶界面形态稳定性是凝聚态物理学和材料科学的一个基础课题^[1-6]. 定向凝固过程中晶体形态的不稳定性可能会导致不同的微观结构, 最终极大地影响产品的物理和机械性能. Hele-Shaw生长室是观察共晶定向凝固过程的典型实验装置, 它是一个封存样品材料的十分扁平的容器. 生长室设置了一个高温区与一个低温区, 高温区的温度设为 T_H , 低温区的温度为 T_C , 材料的凝固温度 T_M 介于两者之间: 即 $T_C < T_M < T_H$. 由于上述温度的设置, 生长室内的样品材料将在高温区处于液态, 在低温区处于固态, 在两个温区之间的某处, 将有一个近似平直的固-液界面. 共晶生长系统具有两个组元(A+B), 组元B在混合熔体中的

浓度用 C 表示. 二元液态混合物被凝固成 α 相和 β 相, 在 α 相中, 组元A是主要成分, 组元B是次要成分; 在 β 相中, 组元B是主要成分, 组元A是次要成分. 多年来, 针对共晶界面形态稳定性有广泛的数值和实验研究. Karma和Sarkissian^[7]利用数值方法发现片层共晶生长主要包含两种震荡稳定模式和一种震荡不稳定模式, 共三种不同类型的稳定模式. 在对称的片层共晶生长中观察到的主要是震荡稳定模式, 在非对称的片层共晶生长中观察到的主要是震荡不稳定模式. Parisi和Plapp^[8]利用三维相场模拟发现锯齿形的不稳定性可能导致片层共晶转化成棒状共晶. Ginibre等^[9]通过实验发现界面倾斜或者震荡将导致新的共晶生长模式. 除了用数值、模拟和实验的方法研究共晶生长形态不稳定性以外, 还有一些研究人员采用解析的方法.

* 国家自然科学基金(批准号: 11401021)资助的课题.

† 通信作者. E-mail: chenmw@ustb.edu.cn

‡ 通信作者. E-mail: wangzd@mater.ustb.edu.cn

Datye 和 Langer^[10] 对共晶生长系统进行线性稳定性分析, 他们假设界面平直从而获得对应问题的特征值. Xu 等^[11-13] 利用渐近分析方法研究了各向同性表面张力作用下共晶生长形态稳定性, 发现片层共晶生长系统包含两种不稳定性机理: “交换稳定性” 机理和 “整体波动不稳定性” 机理.

固体材料本身并非各向同性介质, 其晶格结构使固体体内的物理量以及表面的物理参数依赖于取向, 变为各向异性量. 固体材料这些物理参量的各向异性特征对凝固过程动力学与界面稳定性机理以至对界面微结构图案的形成与选择造成重要的影响^[14]. 王志军等^[15,16] 研究了各向异性表面张力对定向凝固过程中初始平界面稳定性的影响, 发现各向异性表面张力的非线性效应导致界面倾斜生长. Chen 等^[17] 研究了各向异性表面张力对定向凝固过程中球晶生长的影响, 发现在各向异性表面张力作用下, 球晶生长初始阶段部分界面首先向内移动, 达到一定的熔化深度后向外移动. Xu^[18] 研究了各向异性表面张力对定向凝固过程中枝晶生长的影响, 发现当存在各向异性表面张力时, 枝晶系统具有两种不同的整体不稳定性机理: 震荡不稳定性与低频不稳定性. 陈明文等^[19] 研究了各向异性表面张力对定向凝固过程中深胞晶生长的影响, 发现当各向异性表面张力增大时, 深胞晶界面全长增大, 根部低端的曲率半径增大. 本文应用多重变量展开法研究各向异性表面张力条件下定向凝固共晶生长形态稳定性, 揭示了各向异性表面张力对共晶生长不稳定性区域大小的影响.

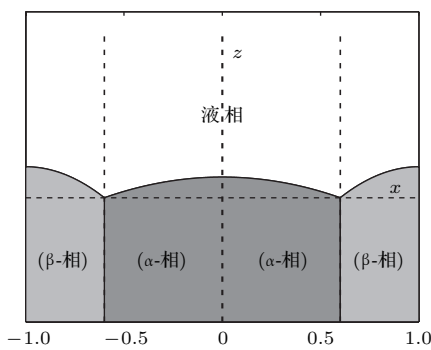


图1 共晶结构的示意图

Fig. 1. Schematic diagram of the eutectic structure.

2 定向凝固系统的数学模型

假设由 α 和 β 两相组成的片层共晶以拉度 V 向液相稳定推进, 共晶片层与固-液界面垂直. 选取

固-液界面处 α 相片层的中心为坐标原点, x 轴与片层垂直, z 轴与晶体生长方向平行, 如图 1 所示. 共晶界面用函数 $z = h(x, t)$ 表示, 它也是共晶生长解的一部分.

本文引用 Xu 等^[12] 的无量纲化尺度, 并且假设主间距的一半 l_w 远小于溶质扩散长度 $l_D = \kappa_D/V$, 即 $l_w \ll l_D$, 其中 κ_D 为溶质扩散系数. 选取 l_w 为长度尺度, V 为速度尺度, l_w/V 为时间尺度, $\Delta H/(c_P \rho_L)$ 为温度尺度, C_e 为浓度尺度, 其中 ΔH 是单位体积内固相潜热, c_P 是比热容, ρ_L 是溶质密度, C_e 是共晶浓度. 无量纲温度 $\bar{T} = (T - T_e)/[\Delta H/(c_P \rho_L)]$, 无量纲浓度 $\bar{C} = (C - C_e)/C_e$, 无量纲无穷远处浓度 $\bar{C}_\infty = [(C_\infty)_D - C_e]/C_e$, 其中 T_e 是共晶温度, $(C_\infty)_D$ 是有量纲无穷远处浓度. 为了书写简洁起见, 下文省略掉无量纲量头上的符号“-”. 各向异性表面张力用四重对称函数 $\gamma(\theta) = \gamma_0[1 + \gamma_4 \cos(4\theta)]$ ^[14] 表示, 其中 γ_0 为各向同性表面张力系数, γ_4 为各向异性表面张力系数, θ 为界面法向量与 z 轴之间的夹角. 共晶生长系统还包含以下无量纲量: Peclet 数 $Pe = l_w/l_D$; 形态参数 $\mathcal{M} = (-mC_e)/[\Delta H/(c_P \rho_L)]$, m 是液相线系数; 界面稳定性参数 $\Gamma = l_c/l_w$, l_c 是毛细长度, $l_c = \gamma_0 c_P \rho_L T_e / (\Delta H)^2$; 无量纲温度梯度 $G = (G)_D l_w / [\Delta H/(c_P \rho_L)]$, $(G)_D$ 是与实验装置相关的有量纲温度梯度; 无量纲间距参数 $W_c = w_c/l_w$, w_c 表示 α 相宽度的一半.

注意到 γ_0 , γ_4 , m 和分离系数 κ 都是分段常值函数, 在 α 相和 β 相都有各自对应的常数值. 用 q 来代表这类物理量, q_α 表示其在 α 相的函数值, q_β 表示其在 β 相的函数值. 由于溶质扩散长度 l_D 远小于热扩散长度 $l_T = \kappa_T/V$, 即 $l_D \ll l_T$, 其中 κ_T 是热扩散系数. 界面温度可以近似表示为 $T_L = T_S \sim G(z - z_*)$, 其中 T_L , T_S 分别是液相和固相温度, z_* 是与 α 相尖端位置有关的常数. 对于典型的实验材料, Peclet 数 Pe 很小. 以 $CBr_4-C_4Cl_6$ ^[20,21] 生长系统为例, $Pe \approx 0.01$, $\Gamma \approx 2.5 \times 10^{-5}$. 为了做渐近分析, 本文把 Peclet 数 Pe 作为基本的小参数, 假设 $\varepsilon = Pe \ll 1$ 且 $\Gamma = \varepsilon^2 \bar{\Gamma}$, $\bar{\Gamma} = O(1)$.

为考察共晶生长形态稳定性, 利用共晶生长的定常解作为基态进行稳定性分析. 在初始时刻 $t = 0$ 时对基态解做一小扰动, 并将在 $t > 0$ 以后形

成的非定常解分解成两个部分:

$$C(x, z, t, \varepsilon) = C_B(x, z, \varepsilon) + \tilde{C}(x, z, t, \varepsilon), \quad (1)$$

$$h(x, t, \varepsilon) = h_B(x, \varepsilon) + \tilde{h}(x, t, \varepsilon), \quad (2)$$

其中 $\{C_B, h_B\}$ 是系统的基态, $\{\tilde{C}, \tilde{h}\}$ 是系统的扰动态. 假设初始扰动态的范数 $\|\tilde{C}(x, z, 0, \varepsilon)\| \ll 1$. 共晶生长系统的定常解为^[11]:

$$C_B = \varpi \hat{C}_\infty (1 - e^{-\varepsilon z}) + \varepsilon \varpi [d_{11,0} e^{-\varepsilon z} + \bar{\Omega}_{11}(x, z)] + \dots, \quad (3)$$

$$h_B(x) \approx \varpi h_{c,0}(x) = \begin{cases} \varpi [\bar{h}_{01,\alpha}(x)(1 - e^{k_{s,\alpha}\hat{x}}) + S_{01} e^{k_{s,\alpha}\hat{x}}], & 0 \leq x < w_0, \\ \varpi [\bar{h}_{01,\beta}(x)(1 - e^{-k_{s,\beta}\hat{x}}) + S_{01} e^{-k_{s,\beta}\hat{x}}], & w_0 < x \leq 1, \end{cases} \quad (4)$$

其中

$$\hat{x} = (x - w_0)/\sqrt{\varepsilon}, \quad w_0 = (\hat{\kappa} - \hat{C}_\infty)/(1 + \hat{\kappa}), \quad C_\infty = \varpi \hat{C}_\infty, \quad \varpi = 1 - \kappa_\alpha, \quad 1 - \kappa_\beta = -\hat{\kappa}\varpi,$$

$$d_{11,0} = \frac{G}{\mathcal{M}_\beta - \mathcal{M}_\alpha} \left(\frac{\hat{s}_1^+}{k_{s,\beta}} - \frac{\hat{s}_1^-}{k_{s,\alpha}} \right) - \hat{P}_{11}(w_0), \quad k_{s,\alpha} = \sqrt{G/\bar{\Gamma}_\alpha}, \quad k_{s,\beta} = \sqrt{G/\bar{\Gamma}_\beta},$$

$$\bar{\Omega}_{11}(x, z) = \sum_{n=1}^{\infty} d_{11,n} \cos(n\pi x) e^{-n\pi z}, \quad d_{11,n} = \frac{2(1 + \hat{\kappa}) \sin(n\pi w_0)}{(n\pi)^2}, \quad \bar{h}_{01,\alpha} = \frac{\mathcal{M}_\alpha}{G} [P_{11}(0) - P_{11}(x)],$$

$$\bar{h}_{01,\beta} = \frac{\mathcal{M}_\alpha}{G} [P_{11}(0) - \frac{\mathcal{M}_\beta}{\mathcal{M}_\alpha} P_{11}(x)], \quad P_{11}(x) = d_{11,0} + \hat{P}_{11}(x), \quad \hat{P}_{11}(x) = \sum_{n=1}^{\infty} \frac{2(1 + \hat{\kappa}) \sin(n\pi w_0)}{(n\pi)^2} \cos(n\pi x),$$

$$S_{01} = \frac{\hat{s}_1^-}{k_{s,\alpha}} + \frac{\mathcal{M}_\alpha}{G} [\hat{P}_{11}(0) - \hat{P}_{11}(w_0)], \quad \hat{s}_1^\pm = \pm \varepsilon^{\frac{1}{2}} \varpi^{-1} \tan \theta^\pm,$$

θ^- 是 α 相的接触角, θ^+ 是 β 相的接触角, 这两个接触角与夹角 $\theta_\alpha, \theta_\beta$ 以及倾斜角 ψ 之间满足关系式 $\theta^- = \theta_\alpha - \pi/2 - \psi, \theta^+ = \theta_\beta - \pi/2 + \psi$, 如图 2 所示.

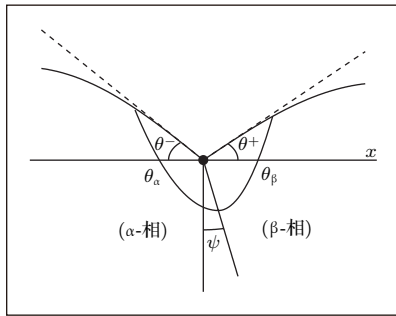


图 2 三相点附近的界面示意图

Fig. 2. A sketch of the interface shape near the triple point.

将系统方程以振幅远小于 1 进行线性化处理, 结合 (1) 式—(4) 式, 可以得到共晶生长系统的扰动态满足以下控制方程和边界条件:

$$\nabla^2 \tilde{C} + \varepsilon \left(\frac{\partial \tilde{C}}{\partial z} - \frac{\partial \tilde{C}}{\partial t} \right) = 0. \quad (5)$$

1) 在远场区域, 当 $z \rightarrow \infty$ 时,

$$\tilde{C}_\infty \rightarrow 0. \quad (6)$$

2) 在侧壁 $x = 0$ 和 $x = 1$ 上,

(a) 对称 (symmetric) 模式 (S-模式)

$$\frac{\partial \tilde{C}}{\partial x} = \frac{\partial \tilde{h}}{\partial x} = 0, \quad (7)$$

(b) 反对称 (antisymmetric) 模式 (A-模式)

$$\tilde{C} = \tilde{h} = 0. \quad (8)$$

3) 在界面 $z = h_B$ 上,

(a) Gibbs-Thomson 条件

$$\begin{aligned} & \tilde{C} + \frac{\partial C_B}{\partial z} \tilde{h} \\ &= -\varepsilon \frac{G}{\mathcal{M}} \tilde{h} + \varepsilon^2 \frac{\bar{\Gamma}(1 - 15\gamma_4 \cos 4\theta)}{\mathcal{M}} \frac{\partial^2 \tilde{h}}{\partial x^2} \\ &+ (\text{h.o.t.}), \end{aligned} \quad (9)$$

由三角诱导公式可知,

$$\begin{aligned} \cos 4\theta &= 2 \cos^2 2\theta - 1 = 2(2 \cos^2 \theta - 1)^2 - 1, \\ \cos^2 \theta &= 1/(1 + \tan^2 \theta), \quad \tan \theta = -h'_B, \end{aligned}$$

于是有

$$\begin{aligned} \cos 4\theta &= 2 \left(\frac{1 - h'^2_B}{1 + h'^2_B} \right)^2 - 1 = 1 - \frac{8h'^2_B}{(1 + h'^2_B)^2}, \\ &1 - 15\gamma_4 \cos 4\theta \\ &= 1 - 15\gamma_4 \left[1 - 8 \left(\frac{h'_B}{1 + h'^2_B} \right)^2 \right] \end{aligned}$$

$$= (1 - 15\gamma_4) + 120\gamma_4 \left(\frac{h'_B}{1 + h'^2_B} \right)^2; \quad (10)$$

结合(9)式和(10)式, Gibbs-Thomson条件可以改写为

$$\begin{aligned} & \tilde{C} + \frac{\partial C_B}{\partial z} \tilde{h} \\ &= -\varepsilon \frac{G}{\mathcal{M}} \tilde{h} + \varepsilon^2 \frac{\bar{\Gamma}}{\mathcal{M}} \left[(1 - 15\gamma_4) \right. \\ & \quad \left. + 120\gamma_4 \left(\frac{h'_B}{1 + h'^2_B} \right)^2 \right] \frac{\partial^2 \tilde{h}}{\partial x^2} + (\text{h.o.t}); \quad (11) \end{aligned}$$

(b) 杂质质量守恒条件

$$\begin{aligned} & \frac{\partial \tilde{C}}{\partial z} + \frac{\partial^2 C_B}{\partial z^2} \tilde{h} - \frac{\partial h_B}{\partial x} \left(\frac{\partial \tilde{C}}{\partial x} + \frac{\partial^2 C_B}{\partial x \partial z} \tilde{h} \right) \\ & + \varepsilon(1 - \kappa) \left(\tilde{C} + \frac{\partial \tilde{h}}{\partial t} + \tan \psi \frac{\partial \tilde{h}}{\partial x} \right) \\ & + (\text{h.o.t}) = 0. \quad (12) \end{aligned}$$

3 扰动态的多重变量渐近展开解

为了得到系统扰动态的渐近解, 引入快变量^[12]

$$\begin{aligned} t_+ &= \frac{t}{\sqrt{\varepsilon}}, \quad x_+ = \frac{1}{\sqrt{\varepsilon}} \int_{w_0}^x k(x_1, z) dx_1, \\ z_+ &= \frac{1}{\sqrt{\varepsilon}} \int_0^z k(x, z_1) dz_1. \quad (13) \end{aligned}$$

按照多重变量 (x, z, x_+, z_+, t_+) , 解可以写成如下形式:

$$\begin{aligned} & \tilde{C}(x, z, x_+, z_+, t_+) \\ &= \varepsilon [\tilde{C}_0(x, z, x_+, z_+) + \sqrt{\varepsilon} \tilde{C}_1(x, z, x_+, z_+)] e^{\sigma(\varepsilon)t_+} \\ & + \dots, \quad (14) \end{aligned}$$

$$\begin{aligned} & \tilde{h}(x, x_+, t_+) \\ &= [\tilde{h}_0(x, x_+) + \sqrt{\varepsilon} \tilde{h}_1(x, x_+)] e^{\sigma(\varepsilon)t_+} + \dots. \quad (15) \end{aligned}$$

并对波数函数和特征值做如下展开:

$$k(x, 0) = \hat{k}(x) = \hat{k}_0(x) + \sqrt{\varepsilon} \hat{k}_1(x) + \dots, \quad (16)$$

$$\sigma(\varepsilon) = \sigma_0 + \sqrt{\varepsilon} \sigma_1 + \dots. \quad (17)$$

3.1 零级近似解

将(13)式—(17)式代入到方程和边界条件(5)式—(12)式, 可以得到系统在零级近似下的控制方程和边界条件为

$$\frac{\partial^2 \tilde{C}_0}{\partial x_+^2} + \frac{\partial^2 \tilde{C}_0}{\partial z_+^2} = 0. \quad (18)$$

1) 在远场区域, 当 $z \rightarrow \infty$ 时,

$$\tilde{C}_0 \rightarrow 0. \quad (19)$$

2) 在侧壁 $x = 0$ 和 $x = 1$ 上,

(a) S-模式

$$\frac{\partial \tilde{C}_0}{\partial x} = \frac{\partial \tilde{h}_0}{\partial x} = 0; \quad (20)$$

(b) A-模式

$$\tilde{C}_0 = \tilde{h}_0 = 0. \quad (21)$$

3) 在界面 $z = 0$ 或 $z_+ = 0$ 上,

(a) Gibbs-Thomson条件

$$\begin{aligned} & \tilde{C}_0 - \varpi \hat{\Theta}(x) \tilde{h}_0 \\ &= -\frac{G}{\mathcal{M}} \tilde{h}_0 + \frac{\bar{\Gamma} \hat{k}_0^2}{\mathcal{M}} \left[(1 - 15\gamma_4) \right. \\ & \quad \left. + 120\gamma_4 \left(\frac{h'_B}{1 + h'^2_B} \right)^2 \right] \frac{\partial^2 \tilde{h}_0}{\partial x_+^2}; \quad (22) \end{aligned}$$

(b) 杂质质量守恒条件

$$\begin{aligned} & \hat{k}_0 \frac{\partial \tilde{C}_0}{\partial z_+} - \varpi \hat{k}_0 h'_{c,0} \frac{\partial \tilde{C}_0}{\partial x_+} \\ & + \varpi \hat{\Theta}(x) \left(\sigma_0 \tilde{h}_0 + \hat{k}_0 \tan \psi \frac{\partial \tilde{h}_0}{\partial x_+} \right) = 0, \quad (23) \end{aligned}$$

其中 $\hat{\Theta}(x)$ 为分段常值函数, $\hat{\Theta}_\alpha = 1$, $\hat{\Theta}_\beta = -\hat{\kappa}$.

4) 三相点处的连接条件, 当 $x = w_0$ 时,

$$\tilde{h}_{0,\alpha} = \tilde{h}_{0,\beta},$$

$$\hat{k}_{0,\alpha} \frac{\partial \tilde{h}_{0,\alpha}}{\partial x_+} = \hat{k}_{0,\beta} \left(\frac{\cos \theta^+}{\cos \theta^-} \right)^2 \frac{\partial \tilde{h}_{0,\beta}}{\partial x_+}. \quad (24)$$

上述共晶生长系统有如下零级近似模式解^[12]:

$$\tilde{C}_0(x, x_+, z, z_+) = \tilde{A}_0(x, z) e^{i x_+ - z_+}, \quad (25)$$

$$\tilde{h}_0(x, x_+) = \hat{D}_0 e^{i x_+}, \quad (26)$$

其中系数 \hat{D}_0 是一个任意的复常数. 记 $\hat{A}_0(x) = \tilde{A}_0(x, 0)$, 将模式解(25)式和(26)式代入到界面条件(22)式和(23)式中, 得到

$$\begin{aligned} & \hat{A}_0(x) + \left\{ -\varpi \hat{\Theta}(x) + \frac{G}{\mathcal{M}} + \frac{\bar{\Gamma} \hat{k}_0^2}{\mathcal{M}} \left[(1 - 15\gamma_4) \right. \right. \\ & \quad \left. \left. + 120\gamma_4 \left(\frac{\varpi h'_{c,0}}{1 + \varpi^2 h'^2_{c,0}} \right)^2 \right] \right\} \hat{D}_0 = 0, \quad (27) \end{aligned}$$

$$\begin{aligned} & (-1 - i\varpi h'_{c,0}) \hat{k}_0 \hat{A}_0(x) \\ & + \varpi \hat{\Theta}(x) (\sigma_0 + i \hat{k}_0 \tan \psi) \hat{D}_0 = 0. \quad (28) \end{aligned}$$

该系统存在非零解的条件是方程的系数行列式为零, 此条件给出了一个局部的色散关系式:

$$(\sigma_0 + i \hat{k}_0 \tan \psi) = \sum (\hat{k}_0, x)$$

$$= \Lambda_0 \hat{k}_0 [\varpi \mathcal{M} \hat{\Theta}(x) - G - \bar{\Gamma}(1 - 15\gamma_4 + 120\gamma_4 \Lambda_1) \hat{k}_0^2], \quad (29)$$

其中

$$\Lambda_0(x) = \frac{1 + i\varpi h'_{c,0}}{\varpi \hat{\Theta}(x) \mathcal{M}},$$

$$\Lambda_1(x) = \left[\frac{\varpi h'_{c,0}(x)}{1 + \varpi^2 h'^2_{c,0}(x)} \right]^2. \quad (30)$$

局部色散关系式 (29) 是定向凝固中, 对于平直界面

情形的 Mullins-Sekerka 公式 [22] 的推广. 当 $\gamma_4 = 0$, $\psi = 0$ 时, (29) 式变为

$$\sigma_0 = \sum (\hat{k}_0, x) = \Lambda_0 \hat{k}_0 [\varpi \mathcal{M} \hat{\Theta}(x) - G - \bar{\Gamma} \hat{k}_0^2], \quad (31)$$

(31) 式与文献 [12] 中给出的 (10) 式相同. 对于任意给定的参数 σ_0 , 从色散关系式 (29) 中可以解出 3 个波函数:

$$\hat{k}_0^{(1)}(x, \gamma_4) = M(x, \gamma_4) \cos \left\{ \frac{1}{3} \arccos \left(\frac{\sigma_0}{\Lambda_0(x) N(x, \gamma_4)} \right) \right\}, \text{ 短波分支,}$$

$$\hat{k}_0^{(2)}(x, \gamma_4) = M(x, \gamma_4) \cos \left\{ \frac{1}{3} \arccos \left(\frac{\sigma_0}{\Lambda_0(x) N(x, \gamma_4)} \right) + \frac{2\pi}{3} \right\},$$

$$\hat{k}_0^{(3)}(x, \gamma_4) = M(x, \gamma_4) \cos \left\{ \frac{1}{3} \arccos \left(\frac{\sigma_0}{\Lambda_0(x) N(x, \gamma_4)} \right) + \frac{4\pi}{3} \right\}, \text{ 长波分支,} \quad (32)$$

其中

$$M(x, \gamma_4) = \sqrt{\frac{4}{3} \left\{ \varpi \mathcal{M} \hat{\Theta}(x) - G - \frac{i \tan \psi}{\Lambda_0} \right\} / \bar{\Gamma} [(1 - 15\gamma_4) + 120\gamma_4 \Lambda_1]},$$

$$N(x, \gamma_4) = -\sqrt{\frac{4}{27\bar{\Gamma} [(1 - 15\gamma_4) + 120\gamma_4 \Lambda_1]} \left\{ \varpi \mathcal{M} \hat{\Theta}(x) - G - \frac{i \tan \psi}{\Lambda_0} \right\}^{3/2}}.$$

当 $\gamma_4 = 0$, $\psi = 0$ 时, (32) 式变为

$$\hat{k}_0^{(1)}(x) = M \cos \left\{ \frac{1}{3} \arccos \left(\frac{\sigma_0}{\Lambda_0 N} \right) \right\}, \quad (33a)$$

$$\hat{k}_0^{(3)}(x) = M \cos \left\{ \frac{1}{3} \arccos \left(\frac{\sigma_0}{\Lambda_0 N} \right) + \frac{4\pi}{3} \right\}, \quad (33b)$$

其中

$$M = \sqrt{\frac{4}{3} \left\{ \varpi \mathcal{M} \hat{\Theta}(x) - G \right\} / \bar{\Gamma}},$$

$$N = -\sqrt{\frac{4}{27\bar{\Gamma}} \left\{ \varpi \mathcal{M} \hat{\Theta}(x) - G \right\}^{3/2}}.$$

(33) 式与 Xu 等 [12] 给出的 (12) 式相同.

这 3 个波函数 $\{\hat{k}_0^{(1)}(x), \hat{k}_0^{(2)}(x), \hat{k}_0^{(3)}(x)\}$ 分别给出了系统 3 个基本的波动形式解 $\{H_1, H_2, H_3\}$. 在这 3 个解中, 波数函数 $\hat{k}_0^{(2)}(x)$ 对应的波动形式解 H_2 必须排除掉, 因为当 $z_+ \rightarrow \infty$ 时, 浓度场的扰动振幅将指数增长, 这是不合理的. 有物理意义的解只有 H_1 和 H_3 . 对于任意固定的点, 在 $\varepsilon \rightarrow 0$ 的极限条件下扰动态的一般解必定是解 H_1 与解 H_3 的线性迭加. 从而, 界面函数外部区域的通解可用这两个基本界面行波的组合表示:

$$\tilde{h}_0(x, \gamma_4) = D_0^{(1)} H_1 + D_0^{(3)} H_3$$

$$= \begin{cases} D_{0,\alpha}^{(1)} e^{i/\sqrt{\varepsilon} \int_{w_0}^x \hat{k}_{0,\alpha}^{(1)}(x_1, \gamma_{4\alpha}) dx_1} + D_{0,\alpha}^{(3)} e^{i/\sqrt{\varepsilon} \int_{w_0}^x \hat{k}_{0,\alpha}^{(3)}(x_1, \gamma_{4\alpha}) dx_1}, & 0 \leq x < w_0, \\ D_{0,\beta}^{(1)} e^{i/\sqrt{\varepsilon} \int_{w_0}^x \hat{k}_{0,\beta}^{(1)}(x_1, \gamma_{4\beta}) dx_1} + D_{0,\beta}^{(3)} e^{i/\sqrt{\varepsilon} \int_{w_0}^x \hat{k}_{0,\beta}^{(3)}(x_1, \gamma_{4\beta}) dx_1}, & w_0 \leq x \leq 1, \end{cases} \quad (34)$$

其中系数 $D_{0,\alpha}^{(1)}, D_{0,\alpha}^{(3)}, D_{0,\beta}^{(1)}, D_{0,\beta}^{(3)}$ 是待定常数.

3.2 一级近似解

浓度场满足的一级近似控制方程和边界条件为:

$$\frac{\partial^2 \tilde{C}_1}{\partial x_+^2} + \frac{\partial^2 \tilde{C}_1}{\partial z_+^2} = 0. \quad (35)$$

1) 在远场区域, 当 $z \rightarrow \infty$ 时,

$$\tilde{C}_1 \rightarrow 0. \quad (36)$$

2) 在侧壁 $x = 0$ 和 $x = 1$ 上,

(a) S-模式

$$\frac{\partial \tilde{C}_1}{\partial x} = \frac{\partial \tilde{h}_1}{\partial x} = 0; \quad (37)$$

(b) A-模式

$$\tilde{C}_1 = \tilde{h}_1 = 0. \quad (38)$$

3) 在界面 $z = 0$ 或 $z_+ = 0$ 上,

(a) Gibbs-Thomson 条件

$$\begin{aligned} & \tilde{C}_1 - \varpi \hat{\Theta}(x) \tilde{h}_1 \\ &= -\frac{G}{\mathcal{M}} \tilde{h}_1 + \frac{2\hat{k}_0 \hat{k}_1 \bar{\Gamma}}{\mathcal{M}} [(1 - 15\gamma_4) + 120\gamma_4 A_1] \frac{\partial^2 \tilde{h}_0}{\partial x_+^2} \\ &+ \frac{\hat{k}_0^2 \bar{\Gamma}}{\mathcal{M}} [(1 - 15\gamma_4) + 120\gamma_4 A_1] \frac{\partial^2 \tilde{h}_1}{\partial x_+^2}; \quad (39) \end{aligned}$$

(b) 杂质质量守恒条件

$$\begin{aligned} & \hat{k}_0 \frac{\partial \tilde{C}_1}{\partial z_+} + \hat{k}_1 \frac{\partial \tilde{C}_0}{\partial z_+} - \varpi h'_{c,0} \left(\hat{k}_0 \frac{\partial \tilde{C}_1}{\partial x_+} + \hat{k}_1 \frac{\partial \tilde{C}_0}{\partial x_+} \right) \\ &+ \varpi \hat{\Theta}(x) \left[\sigma_0 \tilde{h}_1 + \sigma_1 \tilde{h}_0 \right. \\ &+ \left. \tan \psi \left(\hat{k}_0 \frac{\partial \tilde{h}_1}{\partial x} + \hat{k}_1 \frac{\partial \tilde{h}_0}{\partial x} \right) \right] = 0. \quad (40) \end{aligned}$$

上述浓度场的一级近似系统是非齐次的, 它允许以下形式的模式解:

$$\tilde{C}_1(x, x_+, z, z_+) = \tilde{A}_1(x, z) e^{ix_+ - z_+}, \quad (41)$$

$$\tilde{h}_1(x, x_+) = \hat{D}_1 e^{ix_+}, \quad (42)$$

其中系数 \hat{D}_1 是一个任意的复常数. 记 $\hat{A}_1(x) = \tilde{A}_1(x, 0)$, 将模式解 (41) 式和 (42) 式代入到界面条

件 (39) 式和 (40) 中, 整理得

$$\begin{aligned} & \hat{A}_1 + \left[-\varpi \hat{\Theta}(x) + \frac{G}{\mathcal{M}} \right. \\ & \left. + \frac{\hat{k}_0^2 \bar{\Gamma} (1 - 15\gamma_4 + 120\gamma_4 A_1)}{\mathcal{M}} \right] \hat{D}_1 = I_1 \hat{D}_0, \quad (43) \end{aligned}$$

$$\begin{aligned} & (-1 - i\varpi h'_{c,0}) \hat{k}_0 \hat{A}_1 \\ &+ \varpi \hat{\Theta}(x) (\sigma_0 + i\hat{k}_0 \tan \psi) \hat{D}_1 = I_2 \hat{D}_0, \quad (44) \end{aligned}$$

其中

$$I_1 = \frac{-2\hat{k}_0 \hat{k}_1 \bar{\Gamma} (1 - 15\gamma_4 + 120\gamma_4 A_1)}{\mathcal{M}}, \quad (45)$$

$$\begin{aligned} I_2 = & (1 + i\varpi h'_{c,0}) \left[\varpi \hat{\Theta}(x) - \frac{G}{\mathcal{M}} \right. \\ & \left. - \frac{\hat{k}_0^2 \bar{\Gamma} (1 - 15\gamma_4 + 120\gamma_4 A_1)}{\mathcal{M}} \right] \hat{k}_1 \\ & - \varpi \hat{\Theta}(x) (\sigma_1 + i\hat{k}_1 \tan \psi). \quad (46) \end{aligned}$$

由于 (43) 式和 (44) 式构成的非齐次线性系统的系数行列式为零, 故 $\{\hat{A}_1, \hat{D}_1\}$ 存在非零解的充分必要条件为

$$\Delta = \det \begin{pmatrix} 1 & I_1 \\ -\hat{k}_0(1 + i\varpi h'_{c,0}) & I_2 \end{pmatrix} = 0, \quad (47)$$

(47) 式给出了共晶生长系统的可解性条件:

$$I_2 + \hat{k}_0(1 + i\varpi h'_{c,0}) I_1 = 0. \quad (48)$$

从方程 (43) 式—(48) 式得到如下公式:

$$\sigma_1 = \frac{\hat{k}_1(x, \gamma_4) \left\{ (1 + i\varpi h'_{c,0}) \left[\varpi \hat{\Theta}(x) - \frac{G}{\mathcal{M}} - \frac{3\hat{k}_0^2 \bar{\Gamma} (1 - 15\gamma_4 + 120\gamma_4 A_1)}{\mathcal{M}} \right] - i\varpi \Theta(x) \tan \psi \right\}}{\varpi \hat{\Theta}(x)}. \quad (49)$$

4 全局模式解和量子化条件

为了得到全局模式解, 界面函数的通解必须要在三相点 $x = w_0$ 处满足连接条件, 在侧壁 $x = 0$ 和 $x = 1$ 处满足侧壁条件. 由于局部解在 α 相和 β 相是反对称的 (A-) 或者是对称的 (S-), 存在着四种不同的组合方式, 因此共晶生长系统允许四种类型的全局模式解, 即 AA-, AS-, SA- 和 SS- 模式, 如图 3 所示. 在图 3(a) 中, 全局解在 α 相和 β 相均是反对称的, 称之为 AA- 模式, 即: 当 $x = 0$ 时, $\tilde{h}_\alpha = 0$; 当 $x = 1$ 时, $\tilde{h}_\beta = 0$. 在图 3(b) 中, 全局解在 α 相是反对称的, 而在 β 相是对称的, 称之为 AS- 模式, 即: 当 $x = 0$ 时, $\tilde{h}_\alpha = 0$; 当 $x = 1$ 时,

$\partial \tilde{h}_\beta / \partial x = 0$. 在图 3(c) 中, 全局解在 α 相是对称的, 而在 β 相是反对称的, 称之为 SA- 模式, 即: 当 $x = 0$ 时, $\partial \tilde{h}_\alpha / \partial x = 0$; 当 $x = 1$ 时, $\tilde{h}_\beta = 0$. 在图 3(d) 中, 全局解在 α 相和 β 相均是对称的, 称之为 SS- 模式, 即: 当 $x = 0$ 时, $\partial \tilde{h}_\alpha / \partial x = 0$; 当 $x = 1$ 时, $\partial \tilde{h}_\beta / \partial x = 0$.

1) 全局 AA- 模式

全局解在三相点处满足连接条件, 在侧壁上满足侧壁条件:

$$\begin{aligned} & \tilde{h}_{0,\alpha} |_{x=w_0} = \tilde{h}_{0,\beta} |_{x=w_0}, \\ & \hat{k}_{0,\alpha} \frac{\partial \tilde{h}_{0,\alpha}}{\partial x_+} \Big|_{x=w_0} = \hat{k}_{0,\beta} \left(\frac{\cos \theta^+}{\cos \theta^-} \right)^2 \frac{\partial \tilde{h}_{0,\beta}}{\partial x_+} \Big|_{x=w_0}, \quad (50) \end{aligned}$$

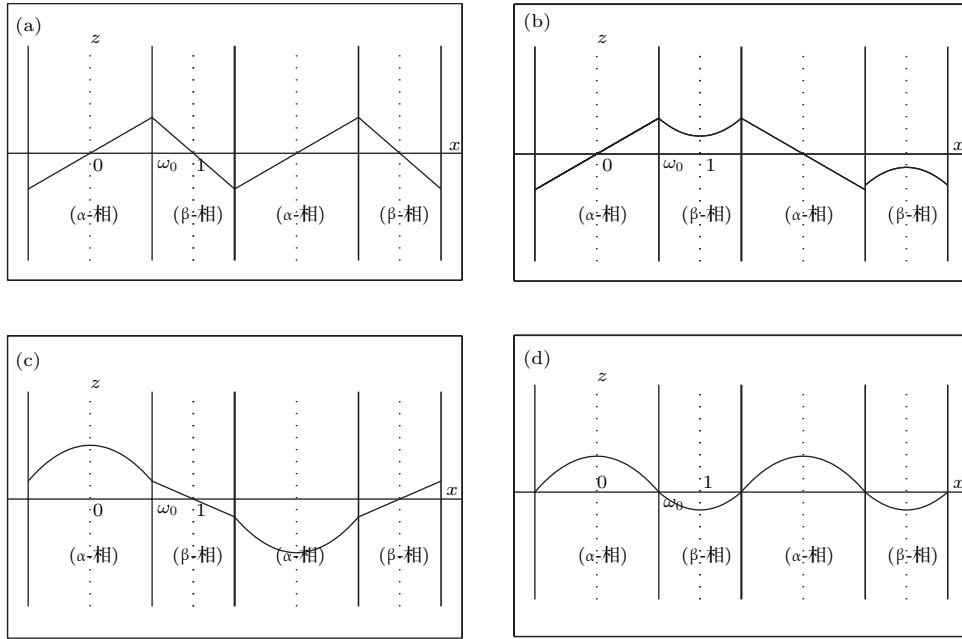


图3 扰动系统的四种振动模式 (a) AA-模式; (b) AS-模式; (c) SA-模式; (d) SS-模式

Fig. 3. Sketch of the perturbed system by four vibration systems connected with a mass: (a) AA-modes; (b) AS-modes; (c) SA-modes; (d) SS-modes.

$$\tilde{h}_{0,\alpha}(0) = 0, \quad \tilde{h}_{0,\beta}(1) = 0. \quad (51)$$

将解(34)式代入到方程(50)式和(51)式中, 常数 $D_{0,\alpha}^{(1)}$, $D_{0,\alpha}^{(3)}$, $D_{0,\beta}^{(1)}$ 和 $D_{0,\beta}^{(3)}$ 满足以下方程组:

$$D_{0,\alpha}^{(1)} + D_{0,\alpha}^{(3)} = D_{0,\beta}^{(1)} + D_{0,\beta}^{(3)}, \quad (52)$$

$$\begin{aligned} & \left(\frac{\cos \theta^-}{\cos \theta^+} \right)^2 [D_{0,\alpha}^{(1)} \hat{k}_{0,\alpha}^{(1)}(w_0) + D_{0,\alpha}^{(3)} \hat{k}_{0,\alpha}^{(3)}(w_0)] \\ &= D_{0,\beta}^{(1)} \hat{k}_{0,\beta}^{(1)}(w_0) + D_{0,\beta}^{(3)} \hat{k}_{0,\beta}^{(3)}(w_0), \end{aligned} \quad (53)$$

$$\begin{aligned} & D_{0,\alpha}^{(1)} e^{\frac{i}{\sqrt{\varepsilon}} \int_{w_0}^0 \hat{k}_{0,\alpha}^{(1)}(x_1, \gamma_{4\alpha}) dx_1} \\ &+ D_{0,\alpha}^{(3)} e^{\frac{i}{\sqrt{\varepsilon}} \int_{w_0}^0 \hat{k}_{0,\alpha}^{(3)}(x_1, \gamma_{4\alpha}) dx_1} = 0, \end{aligned} \quad (54)$$

$$\begin{aligned} & D_{0,\beta}^{(1)} e^{\frac{i}{\sqrt{\varepsilon}} \int_{w_0}^1 \hat{k}_{0,\beta}^{(1)}(x_1, \gamma_{4\beta}) dx_1} \\ &+ D_{0,\beta}^{(3)} e^{\frac{i}{\sqrt{\varepsilon}} \int_{w_0}^1 \hat{k}_{0,\beta}^{(3)}(x_1, \gamma_{4\beta}) dx_1} = 0. \end{aligned} \quad (55)$$

从方程组(52)–(55), 得到

$$D_{0,\alpha}^{(3)} = -D_{0,\alpha}^{(1)} e^{-i\chi_\alpha}, \quad D_{0,\beta}^{(3)} = -D_{0,\beta}^{(1)} e^{-i\chi_\beta}, \quad (56)$$

$$\begin{aligned} & \frac{D_{0,\beta}^{(1)}}{D_{0,\alpha}^{(1)}} = \frac{1 - e^{-i\chi_\alpha}}{1 - e^{-i\chi_\beta}} \\ &= \left(\frac{\cos \theta^-}{\cos \theta^+} \right)^2 \frac{[\hat{k}_{0,\alpha}^{(1)}(w_0) - e^{-i\chi_\alpha} \hat{k}_{0,\alpha}^{(3)}(w_0)]}{[\hat{k}_{0,\beta}^{(1)}(w_0) - e^{-i\chi_\beta} \hat{k}_{0,\beta}^{(3)}(w_0)]}, \end{aligned} \quad (57)$$

其中

$$\chi_\alpha = \frac{1}{\sqrt{\varepsilon}} \int_0^{w_0} [\hat{k}_{0,\alpha}^{(1)}(x_1, \gamma_{4\alpha}) - \hat{k}_{0,\alpha}^{(3)}(x_1, \gamma_{4\alpha})] dx_1,$$

$$\chi_\beta = \frac{-1}{\sqrt{\varepsilon}} \int_{w_0}^1 [\hat{k}_{0,\beta}^{(1)}(x_1, \gamma_{4\beta}) - \hat{k}_{0,\beta}^{(3)}(x_1, \gamma_{4\beta})] dx_1. \quad (58)$$

对于全局AA-模式, 特征值 σ_0 满足以下量子化条件:

$$\frac{1 - e^{-i\chi_\alpha}}{1 - e^{-i\chi_\beta}} = \Xi \frac{[\hat{k}_{0,\alpha}^{(1)}(w_0) - e^{-i\chi_\alpha} \hat{k}_{0,\alpha}^{(3)}(w_0)]}{[\hat{k}_{0,\beta}^{(1)}(w_0) - e^{-i\chi_\beta} \hat{k}_{0,\beta}^{(3)}(w_0)]}, \quad (59)$$

其中 $\Xi = (\cos \theta^- / \cos \theta^+)^2$.

2) 全局AS-模式

全局解在三相点处满足连接条件, 在侧壁上满足侧壁条件:

$$\begin{aligned} & \tilde{h}_{0,\alpha} |_{x=w_0} = \tilde{h}_{0,\beta} |_{x=w_0}, \\ & \hat{k}_{0,\alpha} \frac{\partial \tilde{h}_{0,\alpha}}{\partial x_+} \Big|_{x=w_0} = \hat{k}_{0,\beta} \Xi^{-1} \frac{\partial \tilde{h}_{0,\beta}}{\partial x_+} \Big|_{x=w_0}, \end{aligned} \quad (60)$$

$$\tilde{h}_{0,\alpha}(0) = 0, \quad \frac{\partial \tilde{h}_{0,\beta}}{\partial x} \Big|_{x=1} = 0. \quad (61)$$

将解(34)式代入到方程(60)式和(61)式中, 化简整理后得

$$\begin{aligned} & D_{0,\alpha}^{(3)} = -D_{0,\alpha}^{(1)} e^{-i\chi_\alpha}, \\ & D_{0,\beta}^{(3)} = -D_{0,\beta}^{(1)} e^{-i\chi_\beta} \frac{\hat{k}_{0,\beta}^{(1)}(1)}{\hat{k}_{0,\beta}^{(3)}(1)}, \end{aligned} \quad (62)$$

$$\frac{D_{0,\beta}^{(1)}}{D_{0,\alpha}^{(1)}} = \frac{1 - e^{-i\chi_\alpha}}{[1 - e^{-i\chi_\beta} \hat{k}_{0,\beta}^{(1)}(1) / \hat{k}_{0,\beta}^{(3)}(1)]}$$

$$= \Xi \frac{[\hat{k}_{0,\alpha}^{(1)}(w_0) - e^{-i\chi_\alpha} \hat{k}_{0,\alpha}^{(3)}(w_0)]}{[\hat{k}_{0,\beta}^{(1)}(w_0) - e^{-i\chi_\beta} \hat{k}_{0,\beta}^{(3)}(w_0)] \hat{k}_{0,\beta}^{(1)}(1) / \hat{k}_{0,\beta}^{(3)}(1)}. \quad (63)$$

对于全局AS-模式, 特征值 σ_0 满足以下量子化条件:

$$\begin{aligned} & \frac{1 - e^{-i\chi_\alpha}}{[\hat{k}_{0,\alpha}^{(1)}(w_0) - e^{-i\chi_\alpha} \hat{k}_{0,\alpha}^{(3)}(w_0)]} \\ &= \Xi \frac{[1 - e^{-i\chi_\beta} \hat{k}_{0,\beta}^{(1)}(1) / \hat{k}_{0,\beta}^{(3)}(1)]}{[\hat{k}_{0,\beta}^{(1)}(w_0) - e^{-i\chi_\beta} \hat{k}_{0,\beta}^{(3)}(w_0)] \hat{k}_{0,\beta}^{(1)}(1) / \hat{k}_{0,\beta}^{(3)}(1)}. \end{aligned} \quad (64)$$

3) 全局SA-模式

全局解在三相点处满足连接条件, 在侧壁上满足侧壁条件:

$$\begin{aligned} \tilde{h}_{0,\alpha} |_{x=w_0} &= \tilde{h}_{0,\beta} |_{x=w_0}, \\ \hat{k}_{0,\alpha} \frac{\partial \tilde{h}_{0,\alpha}}{\partial x_+} \Big|_{x=w_0} &= \hat{k}_{0,\beta} \Xi^{-1} \frac{\partial \tilde{h}_{0,\beta}}{\partial x_+} \Big|_{x=w_0}. \end{aligned} \quad (65)$$

$$\frac{\partial \tilde{h}_{0,\alpha}}{\partial x} \Big|_{x=0} = 0, \quad \tilde{h}_{0,\beta}(1) = 0. \quad (66)$$

将解(34)式代入到方程(65)式和(66)式中, 化简整理后得

$$\begin{aligned} D_{0,\alpha}^{(3)} &= -D_{0,\alpha}^{(1)} e^{-i\chi_\alpha} \frac{\hat{k}_{0,\alpha}^{(1)}(0)}{\hat{k}_{0,\alpha}^{(3)}(0)}, \\ D_{0,\beta}^{(3)} &= -D_{0,\beta}^{(1)} e^{-i\chi_\beta}, \\ \frac{D_{0,\beta}^{(1)}}{D_{0,\alpha}^{(1)}} &= \frac{1 - e^{-i\chi_\alpha} \hat{k}_{0,\alpha}^{(1)}(0) / \hat{k}_{0,\alpha}^{(3)}(0)}{1 - e^{-i\chi_\beta}}, \\ &= \Xi \frac{[\hat{k}_{0,\alpha}^{(1)}(w_0) - e^{-i\chi_\alpha} \hat{k}_{0,\alpha}^{(3)}(w_0)] \hat{k}_{0,\alpha}^{(1)}(0) / \hat{k}_{0,\alpha}^{(3)}(0)}{[\hat{k}_{0,\beta}^{(1)}(w_0) - e^{-i\chi_\beta} \hat{k}_{0,\beta}^{(3)}(w_0)]}. \end{aligned} \quad (68)$$

对于全局SA-模式, 特征值 σ_0 满足以下量子化条件:

$$\begin{aligned} & \frac{[1 - e^{-i\chi_\alpha} \hat{k}_{0,\alpha}^{(1)}(0) / \hat{k}_{0,\alpha}^{(3)}(0)]}{[\hat{k}_{0,\alpha}^{(1)}(w_0) - e^{-i\chi_\alpha} \hat{k}_{0,\alpha}^{(3)}(w_0)] \hat{k}_{0,\alpha}^{(1)}(0) / \hat{k}_{0,\alpha}^{(3)}(0)} \\ &= \Xi \frac{1 - e^{-i\chi_\beta}}{[\hat{k}_{0,\beta}^{(1)}(w_0) - e^{-i\chi_\beta} \hat{k}_{0,\beta}^{(3)}(w_0)]}. \end{aligned} \quad (69)$$

4) 全局SS-模式

全局解在三相点处满足连接条件, 在侧壁上满足侧壁条件:

$$\begin{aligned} \tilde{h}_{0,\alpha} |_{x=w_0} &= \tilde{h}_{0,\beta} |_{x=w_0}, \\ \hat{k}_{0,\alpha} \frac{\partial \tilde{h}_{0,\alpha}}{\partial x_+} \Big|_{x=w_0} &= \hat{k}_{0,\beta} \Xi^{-1} \frac{\partial \tilde{h}_{0,\beta}}{\partial x_+} \Big|_{x=w_0}, \end{aligned} \quad (70)$$

$$\frac{\partial \tilde{h}_{0,\alpha}}{\partial x} \Big|_{x=0} = 0, \quad \frac{\partial \tilde{h}_{0,\beta}}{\partial x} \Big|_{x=1} = 0. \quad (71)$$

将解(34)式代入到方程(70)式和(71)式中, 化简整理后得

$$\begin{aligned} D_{0,\alpha}^{(3)} &= -D_{0,\alpha}^{(1)} e^{-i\chi_\alpha} \frac{\bar{k}_{0,\alpha}^{(1)}(0)}{\bar{k}_{0,\alpha}^{(3)}(0)}, \\ D_{0,\beta}^{(3)} &= -D_{0,\beta}^{(1)} e^{-i\chi_\beta} \frac{\bar{k}_{0,\beta}^{(1)}(1)}{\bar{k}_{0,\beta}^{(3)}(1)}, \end{aligned} \quad (72)$$

$$\begin{aligned} \frac{D_{0,\beta}^{(1)}}{D_{0,\alpha}^{(1)}} &= \frac{[1 - e^{-i\chi_\alpha} \hat{k}_{0,\alpha}^{(1)}(0) / \hat{k}_{0,\alpha}^{(3)}(0)]}{[1 - e^{-i\chi_\beta} \hat{k}_{0,\beta}^{(1)}(1) / \hat{k}_{0,\beta}^{(3)}(1)]} \\ &= \Xi \frac{[\hat{k}_{0,\alpha}^{(1)}(w_0) - e^{-i\chi_\alpha} \hat{k}_{0,\alpha}^{(3)}(w_0)] \hat{k}_{0,\alpha}^{(1)}(0) / \hat{k}_{0,\alpha}^{(3)}(0)}{[\hat{k}_{0,\beta}^{(1)}(w_0) - e^{-i\chi_\beta} \hat{k}_{0,\beta}^{(3)}(w_0)] \hat{k}_{0,\beta}^{(1)}(1) / \hat{k}_{0,\beta}^{(3)}(1)}}. \end{aligned} \quad (73)$$

对于全局SS-模式, 特征值 σ_0 满足以下量子化条件:

$$\begin{aligned} & \frac{[1 - e^{-i\chi_\alpha} \hat{k}_{0,\alpha}^{(1)}(0) / \hat{k}_{0,\alpha}^{(3)}(0)]}{[1 - e^{-i\chi_\beta} \hat{k}_{0,\beta}^{(1)}(1) / \hat{k}_{0,\beta}^{(3)}(1)]} \\ &= \Xi \frac{[\hat{k}_{0,\alpha}^{(1)}(w_0) - e^{-i\chi_\alpha} \hat{k}_{0,\alpha}^{(3)}(w_0)] \hat{k}_{0,\alpha}^{(1)}(0) / \hat{k}_{0,\alpha}^{(3)}(0)}{[\hat{k}_{0,\beta}^{(1)}(w_0) - e^{-i\chi_\beta} \hat{k}_{0,\beta}^{(3)}(w_0)] \hat{k}_{0,\beta}^{(1)}(1) / \hat{k}_{0,\beta}^{(3)}(1)}}. \end{aligned} \quad (74)$$

5 稳定性分析

由量子化条件可以看出特征值 σ_0 是关于参数 ε 和 γ_4 的隐函数. 任意给定参数 ε 和 γ_4 , 可以得到一个复数值 σ_0 . 为了更好地阐明生长条件对共晶生长系统的影响, 引入无量纲参数^[11,12] $v = \ell_{c,\alpha} V / \kappa_D$, 它反映拉速 V 的大小; $\hat{\beta} = -\ell_{c,\alpha} (G)_D / m_\alpha C_e$, 它反映温度梯度 $(G)_D$ 的大小. 通过化简可以知道, $v = \varepsilon^3 \bar{\Gamma}_\alpha$, $\hat{\beta} = vG/M$. 本文采用与Xu^[23]研究枝晶的形态稳定性相似的方法, 对于四种震荡模式得到各自对应的稳定临界值 ε_{aa^*} , ε_{as^*} , ε_{sa^*} 和 ε_{ss^*} . 共晶生长系统稳定的选择判据为:

当 $\varepsilon > \varepsilon_{*,\min}$, 共晶生长系统是不稳定的;

当 $\varepsilon \leq \varepsilon_{*,\min}$, 共晶生长系统是稳定的.

共晶生长系统稳定的选择性条件为:

$$\varepsilon = \varepsilon_{*,\min} = \min \{ \varepsilon_{aa^*}, \varepsilon_{as^*}, \varepsilon_{sa^*}, \varepsilon_{ss^*} \}. \quad (75)$$

1) 全局稳定模式

给定生长条件, 令量子化条件(59)式、(64)式、(69)式和(74)式中特征值 $\sigma_0 = 0$, 发现只有AA-模式允许一系列中性稳定曲线, 这种非震荡条件下的不稳定模式又被称为ST-模式. ST-模式导致所谓

的交换稳定性机理. 从图 4 可知, 随着各向异性表面张力系数增大, 稳定临界值 ε_* 随之减小. 这就意味着, 各向异性表面张力减小稳定性区域, 使得交换稳定性机理更加稳定. 当各向异性表面张力退化为各向同性表面张力时, 即当 $\gamma_{4\alpha} = 0, \gamma_{4\beta} = 0$ 时, 图 4(a) 中虚线与 Xu 等 [12] 给出的图 5(a) 中黑色实线一致, 图 4(b) 中实线与 Xu 等 [12] 给出的图 5(b) 中红色实线一致. 对比图 4(a) 中三条曲线, 各向异性表面张力对片层共晶稳定性有显著的影响.

2) 全局震荡模式

给定生长条件, 令量子化条件 (59) 式、(64) 式、(69) 式和 (74) 式中 $\text{Re}(\sigma_0) = 0, \text{Im}(\sigma_0) = \omega_* \neq 0$, 用数值的方法计算 AA-, AS-, SA- 和 SS- 模式对应

的稳定临界值 $\varepsilon_{aa^*}, \varepsilon_{as^*}, \varepsilon_{sa^*}$ 和 ε_{ss^*} . 这四种振荡不稳定模式导致了所谓的全局不稳定性机理, 图 5—图 8 给出了四种震荡不稳定模式的稳定临界值 $\varepsilon_{aa^*}, \varepsilon_{as^*}, \varepsilon_{sa^*}$ 和 ε_{ss^*} 随着 v 的变化图. 从图 5、图 7 和图 8 可以看出, 随着各向异性表面张力系数增大, 稳定临界值 $\varepsilon_{aa^*}, \varepsilon_{sa^*}$ 和 ε_{ss^*} 随之减小. 这就意味着各向异性表面张力减小片层共晶生长的稳定性区域, 增强了 AA-, SA- 和 SS- 这三种全局震荡模式的全局不稳定性; 然而, 对于 AS- 全局震荡模式而言, 从图 6 可以看出, 随着各向异性表面张力系数增大, 稳定临界值 ε_{as^*} 随之增大. 这就意味着, 各向异性表面张力增大片层共晶生长的稳定性区域, 减弱了 AS- 全局震荡模式的全局不稳定性.

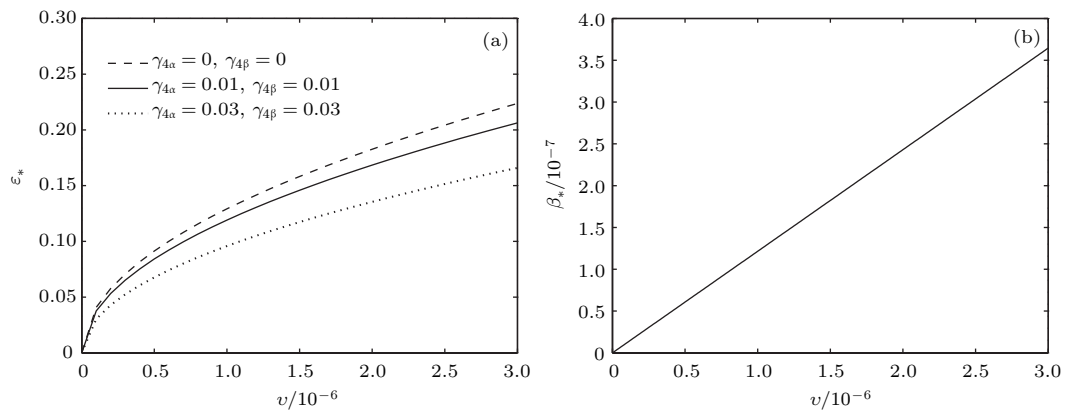


图 4 当 $\sigma_0 = 0$ ($n = 0$) 时, 对于 AA- 模式, 临界值 ε_* 随 v 的变化, 其中 $\hat{C}_\infty = -0.12, w_0 = 0.63, \varpi = 0.15, \hat{\kappa} = 1.33, (R_c = \bar{I}_\beta / \bar{I}_\alpha), \mathcal{M}_\alpha = 0.107, \mathcal{M}_\beta = -0.0711, \theta^+ = 65.3^\circ, \theta^- = 59.5^\circ, \psi = 0, \hat{\beta} = 4.88 \times 10^{-10}$ (a) 临界值 ε_* 随 v 的变化; (b) 参数 β_* 随 v 的变化

Fig. 4. The variation of ε_* with v for the AA-mode when the eigenvalue $\sigma_0 = 0$ ($n = 0$), where $\hat{C}_\infty = -0.12, w_0 = 0.63, \varpi = 0.15, \hat{\kappa} = 1.33, (R_c = \bar{I}_\beta / \bar{I}_\alpha), \mathcal{M}_\alpha = 0.107, \mathcal{M}_\beta = -0.0711, \theta^+ = 65.3^\circ, \theta^- = 59.5^\circ, \hat{\beta} = 4.88 \times 10^{-10}$: (a) The variation of the stability critical number ε_* with v ; (b) the variation of β_* with v .

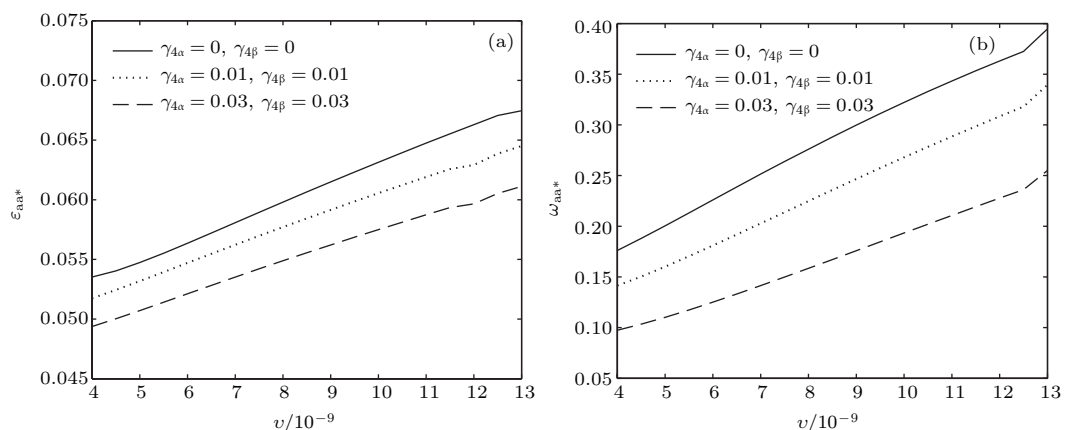


图 5 当 $\text{Re}(\sigma_0) = 0, \text{Im}(\sigma_0) = \omega_{aa^*}$ 时, 对于 AA- 模式, (a) 临界值 ε_{aa^*} 随 v 的变化, (b) 特征频率值 ω_{aa^*} 随 v 的变化, 其他参数取值同图 4

Fig. 5. The variation of ε_{aa^*} with v for the AA-mode when the eigenvalue $\text{Re}(\sigma_0) = 0, \text{Im}(\sigma_0) = \omega_{aa^*}$: (a) The variation of the stability critical number ε_{aa^*} with v ; (b) the variation of the corresponding eigenfrequency ω_{aa^*} with v . The values of other parameters are the same as those given in Fig. 4.

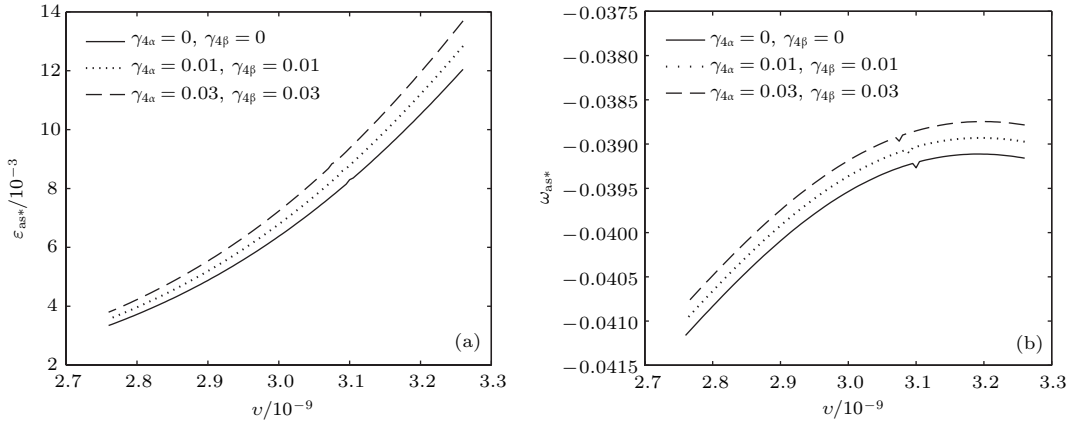


图6 当 $\text{Re}(\sigma_0) = 0, \text{Im}(\sigma_0) = \omega_{\text{as}*}$ 时, 对于 AS-模式, (a) 临界值 $\varepsilon_{\text{as}*}$ 随 ν 的变化, (b) 特征频率值 $\omega_{\text{as}*}$ 随 ν 的变化, 其他参数取值同图4

Fig. 6. The variation of $\varepsilon_{\text{as}*}$ with ν for the AS-mode when the eigenvalue $\text{Re}(\sigma_0) = 0, \text{Im}(\sigma_0) = \omega_{\text{as}*}$: (a) The variation of the stability critical number $\varepsilon_{\text{as}*}$ with ν ; (b) the variation of the corresponding eigenfrequency $\omega_{\text{as}*}$ with ν . The values of other parameters are the same as those given in Fig. 4.

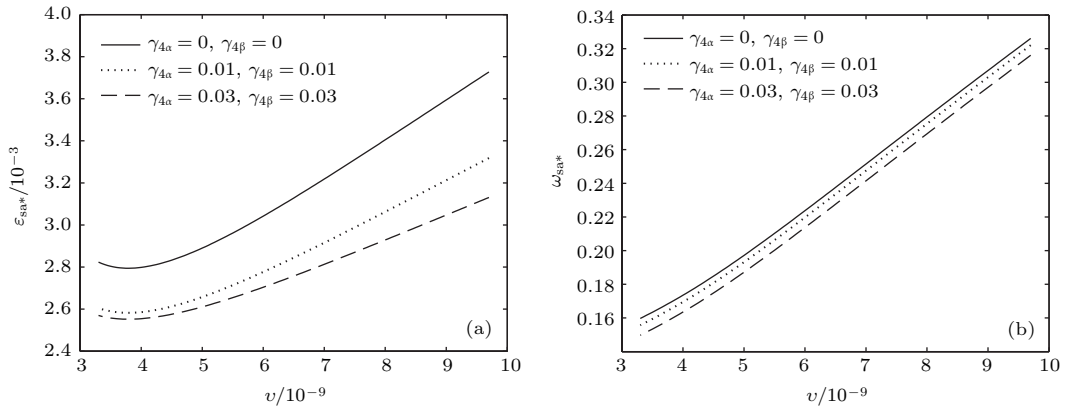


图7 当 $\text{Re}(\sigma_0) = 0, \text{Im}(\sigma_0) = \omega_{\text{sa}*}$ 时, 对于 SA-模式, (a) 临界值 $\varepsilon_{\text{sa}*}$ 随 ν 的变化, (b) 特征频率值 $\omega_{\text{sa}*}$ 随 ν 的变化, 其他参数取值同图4

Fig. 7. The variation of $\varepsilon_{\text{sa}*}$ with ν for the SA-mode when the eigenvalue $\text{Re}(\sigma_0) = 0, \text{Im}(\sigma_0) = \omega_{\text{sa}*}$: (a) The variation of the stability critical number $\varepsilon_{\text{sa}*}$ with ν ; (b) the variation of the corresponding eigenfrequency $\omega_{\text{sa}*}$ with ν . The values of other parameters are the same as those given in Fig. 4.

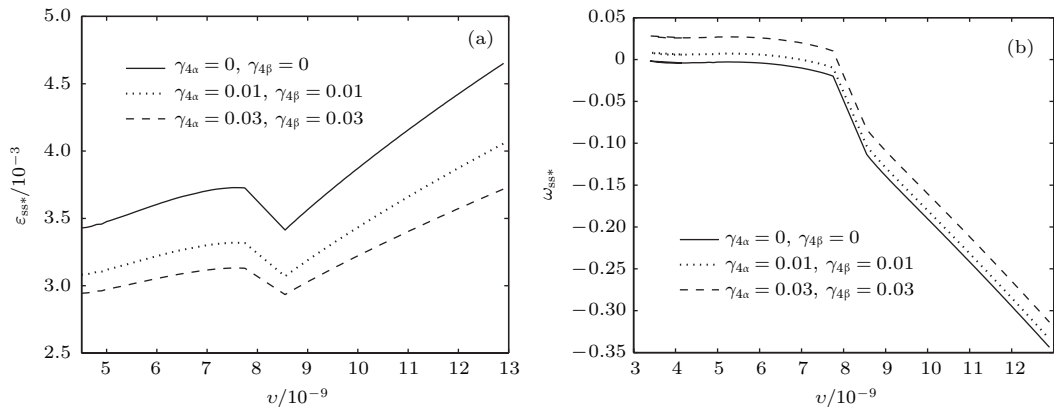


图8 当 $\text{Re}(\sigma_0) = 0, \text{Im}(\sigma_0) = \omega_{\text{ss}*}$ 时, 对于 SS-模式, (a) 临界值 $\varepsilon_{\text{ss}*}$ 随 ν 的变化, (b) 特征频率值 $\omega_{\text{ss}*}$ 随 ν 的变化, 其他参数取值同图4

Fig. 8. The variation of $\varepsilon_{\text{ss}*}$ with ν for the SS-mode when the eigenvalue $\text{Re}(\sigma_0) = 0, \text{Im}(\sigma_0) = \omega_{\text{ss}*}$: (a) The variation of the stability critical number $\varepsilon_{\text{ss}*}$ with ν ; (b) the variation of the corresponding eigenfrequency $\omega_{\text{ss}*}$ with ν . The values of other parameters are the same as those given in Fig. 4.

6 结 论

本文研究了定向凝固过程中各向异性表面张力对共晶生长形态稳定性的影响. 应用多重变量渐近展开法解决了表面张力为各向异性时线性绕动态的特征值问题, 导出了受各向异性表面张力影响的界面形态表达式和扰动振幅变化率与波数满足的色散关系, 以此为基础给出了共晶生长的临界稳定性判据和界面形态满足的量子化条件. 结果表明: 各向异性表面张力对定向凝固系统的稳定性有显著的影响. 与各向同性表面张力条件下的共晶凝固系统相比较, 考虑各向异性表面张力的定向凝固系统中共晶生长界面形态也有两种整体不稳定机理: 由非震荡导致的“交换稳定性”和由震荡导致的“整体波动不稳定性”机理. 稳定性分析表明共晶界面稳定性取决于 Peclet 数的某一个临界值 ε_* , 当 Peclet 数大于临界值 ε_* 时, 共晶界面形态不稳定; 当 Peclet 数小于临界值 ε_* 时, 共晶界面形态稳定. 随着各向异性表面张力增大, 对应于 AA-, SA-和 SS-模式的临界值 ε_{aa^*} , ε_{as^*} , ε_{sa^*} 和 ε_{ss^*} 减小, 各向异性表面张力减小稳定性区域, 各向异性表面张力加强这三种模式的稳定性; 然而, 随着各向异性表面张力增大, 对应于 AS-模式的临界值 ε_{as^*} 也增大, 各向异性表面张力增大稳定性区域, 各向异性表面张力减弱 AS-模式的稳定性.

本文得到了加拿大麦吉尔大学徐鉴君教授的指导与帮助, 作者表示感谢. 作者徐小花感谢天津城建大学陈永强教授的有益讨论与帮助.

参考文献

- [1] Jackson K A, Hunt J D 1966 *Trans. Metall. Soc. AIME* **236** 1129
- [2] Trivedi R, Mangin P, Kurz W 1987 *Acta Metall.* **35** 971
- [3] Liu J M, Zhou Y H, Shang B L 1990 *Acta Metall. Mater.* **38** 1625
- [4] Kassner K, Misbah C 1991 *Phys. Rev. A* **44** 6533
- [5] Li X, Ren Z M, Fautrelle Y, Zhang Y D, Esling C 2010 *Acta Mater.* **58** 1403
- [6] Meng G H, Lin X, Huang W D 2007 *J. Mater. Sci. Technol.* **23** 851
- [7] Karma A, Sarkissian A 1996 *Metall. Mater. Trans. A* **27** 635
- [8] Parisi A, Plapp M 2008 *Acta Mater.* **56** 1348
- [9] Ginibre M, Akamatsu S, Faivre G 1997 *Phys. Rev. E* **56** 780
- [10] Datye V, Langer J S 1981 *Phys. Rev. B* **24** 4155
- [11] Xu J J, Li X M, Chen Y Q 2014 *J. Cryst. Growth* **401** 93
- [12] Xu J J, Chen Y Q, Li X M 2014 *J. Cryst. Growth* **401** 99
- [13] Xu J J 2017 *Interfacial Wave Theory of Pattern Formation in Solidification: Dendrites, Fingers, Cells and Free Boundaries* (2nd Ed.) (New York: Springer) pp503–572
- [14] Xu J J 2006 *Introduction to kinetics of solidification and stability theory of the interface* (Beijing: Science Press) pp33–44 (in Chinese) [徐鉴君 2006 凝固过程动力学与界面稳定性理论导引 (北京: 科学出版社) 第 33—44 页]
- [15] Wang Z J, Wang J C, Yang G C 2008 *Acta Phys. Sin.* **57** 1246 (in Chinese) [王志军, 王锦程, 杨根仓 2008 物理学报 **57** 1246]
- [16] Wang Z J, Wang J C, Yang G C 2010 *Chin. Phys. B* **19** 017305
- [17] Chen M W, Wang Z D, Xu J J 2014 *J. Cryst. Growth* **385** 115
- [18] Xu J J 1991 *Physica D* **51** 579
- [19] Chen M W, Chen Y C, Zhang W L, Liu X M, Wang Z D 2014 *Acta Phys. Sin.* **63** 038101 (in Chinese) [陈明文, 陈奕臣, 张文龙, 刘秀敏, 王自东 2014 物理学报 **63** 038101]
- [20] Seetharaman V, Trivedi R 1988 *Metall. Trans. A* **19** 2955
- [21] Mergy J, Faivre G, Guthmann C, Mellet R 1993 *J. Cryst. Growth* **134** 353
- [22] Mullins W W, Sekerka R F 1964 *J. Appl. Phys.* **35** 444
- [23] Xu J J 2002 *J. Cryst. Growth* **245** 134

Effect of anisotropic surface tension on morphological stability of lamellar eutectic growth in directional solidification*

Xu Xiao-Hua¹⁾ Chen Ming-Wen^{1)†} Wang Zi-Dong^{2)‡}

1) (School of Mathematics and Physics, University of Science and Technology Beijing, Beijing 100083, China)

2) (School of Materials Science and Engineering, University of Science and Technology Beijing, Beijing 100083, China)

(Received 25 January 2018; revised manuscript received 15 March 2018)

Abstract

Lamellar eutectic solidification is very important in the development of new materials in which the periodic multiphase structures each may have a remarkable or enhanced functionality. The morphological instability during solidification may lead to various eutectic microstructures and greatly affect the physical and mechanical properties of final solidification products. In this paper, the morphological stability of lamellar eutectic growth with the anisotropic surface tension is studied by using the matched asymptotic expansion method and multiple variable expansion method. We assume that the process of solidification is viewed as a two-dimensional problem, The anisotropic surface tension is a four-fold symmetry function. The solute diffusion in the solid phase is negligible, and there is no convection in the system. On the basis of the basic state solution for the lamellar eutectic in directional solidification, the asymptotic solution for the perturbed interface shape of lamellar eutectic growth under the anisotropic surface tension is obtained in the case where the Peclet number is small, and then the quantization conditions of interfacial morphology for lamellar eutectic crystal is obtained. A dispersion relation between the wave number and the perturbation amplification rate, and the stability criterion of lamellar eutectic growth under the anisotropic surface tension are also obtained.

The result shows that the anisotropic surface tension has a significant effect on lamellar eutectic growth in directional solidification. It shows that comparing the directional solidification system of isotropic surface tension, the interface morphological stability of anisotropic surface tension also involves two types of global instability mechanisms: the ‘exchange of stability’ induced by the non-oscillatory, unstable modes and the global wave instability caused by four types of oscillatory unstable modes, namely antisymmetric antisymmetric (AA)-, symmetric antisymmetric (SA)-, antisymmetric symmetric (AS)-, and symmetric symmetric (SS)- modes. The linear stability analysis reveals that the stability of lamellar eutectic growth depends on stability critical number ε_* . When $\varepsilon > \varepsilon_*$, the eutectic growth system is unstable; When $\varepsilon \leq \varepsilon_*$, the eutectic growth system is stable. The anisotropic surface tension, by reducing the corresponding stability critical number ε_* , stabilizes both the ‘exchange of stability’ mechanism and the global instability mechanism for the AA-, SA- and SS-modes. It implies that the anisotropic surface tension parameter tends to reduce the stability zone. However, by increasing the corresponding stability critical number ε_* , the anisotropic surface tension destabilizes the global instability mechanism for the AS-mode. It implies that the anisotropic surface tension parameter tends to increase the stability zone for AS-mode.

Keywords: directional solidification, eutectic growth, anisotropic surface tension, morphological stability

PACS: 81.10.Aj, 68.03.Cd, 68.08.-p, 81.30.Fb

DOI: 10.7498/aps.67.20180186

* Project supported by the National Natural Science Foundation of China (Grant No. 11401021).

† Corresponding author. E-mail: chenmw@ustb.edu.cn

‡ Corresponding author. E-mail: wangzd@mater.ustb.edu.cn